# A Study on the "Runaway Greenhouse Effect" with a One-Dimensional Radiative–Convective Equilibrium Model

SHINICHI NAKAJIMA

*Space Development Division, NEC Corporation, Midori, Yokohama, Japan*

YOSHI-YUKI HAYASHI

*Department of Earth and Planetary Physics, Faculty of Science, University of Tokyo, Bunkyo, Tokyo, Japan*

YUTAKA ABE*

*Water Research Institute, Nagoya University, Furou-cho, Chikusa, Nagoya, Japan*

(Manuscript received 14 March 1991, in final form 17 January 1992)

ABSTRACT

A simple one-dimensional radiative–convective equilibrium model is used to investigate the relationship between the surface temperature and the outgoing infrared radiation at the top of the atmosphere. The model atmosphere has a gray infrared absorption coefficient and is composed of a radiative equilibrium stratosphere and a moist adiabat troposphere.

An upper limit of the outgoing infrared radiation is found to exist. The existence of the upper limit is characterized by the radiation limits that appear when the optical depth of the entire atmosphere becomes sufficiently deep and the temperature structure around the levels where the optical depth is about unity approaches a fixed profile. This appearance of an upper limit differs from that found by Komabayashi and Ingersoll, which is obtained from the constraint of the stratospheric radiation balance.

As one of those radiation limits, the outgoing infrared radiation has an asymptotic limit as the surface temperature increases. This is caused by the tropospheric structure approaching the water vapor saturation curve. It is considered that the asymptotic limits appearing in the radiatively and thermodynamically more complicated models utilized by Abe and Matsui and Kasting are corresponding to this asymptotic limit indicated in our model.

## 1. Introduction

The problem of whether or not the oceans would evaporate plays an important role in studying the evolution of atmospheres of terrestrial planets. It has been suggested that, since water vapor is a very efficient infrared absorber and its saturation vapor pressure is a rapidly increasing function of temperature, the oceans would evaporate rather easily by the so-called runaway greenhouse effect (e.g., Plass 1961; Gold 1964). We can imagine an unstable process in the following way. Let us assume a situation where the incident solar flux into the atmosphere $F_0$ is slightly increased. As $F_0$ rises, the surface temperature $T_s$ will also increase. The higher $T_s$ will cause a large increase in the water vapor supply. As a result, the mass of the infrared absorber will make a great gain, and to obtain an increase in $F^{\uparrow}_{\mathrm{IRtop}}$, the outgoing infrared radiation at the top of the atmosphere, which should balance with the original increase in $F_0$, $T_s$ will have to become even higher. The increase of $T_s$ will cause a further supply of water vapor that will cause $T_s$ to rise farther. It is expected that this feedback process will continue until the oceans are completely evaporated.

We have to note, however, that previous studies related to the runaway greenhouse effect (e.g., Komabayashi 1967, 1968; Ingersol 1969; Kasting 1988; Abe and Matsui 1988) did not pursue the dynamic behavior of the atmosphere and did not confirm the existence of the effect as an unstable process, as described above. They considered an atmosphere in an equilibrium state and obtained conditions for the oceans to exist under it. In order to distinguish those steady-state considerations from the instability idea of Plass (1961) and Gold (1964), the atmospheric state where the ocean cannot exist in an equilibrium state will be referred to as an atmosphere in a *runaway greenhouse state.*

* *Present affiliation:* Department of Earth and Planetary Physics, Faculty of Science, University of Tokyo.

*Corresponding author address:* Dr. Yoshi-Yuki Hayashi, Department of Earth and Planetary Physics, University of Tokyo, Yayoi, Bunkyo-ku, Tokyo 113, Japan.

The purpose of this paper is to investigate the atmospheric structures that cause the runaway greenhouse state. We have to make another note, however, before approaching this problem. We can distinguish three cases of seawater evaporation in an equilibrium state (Abe 1988). The first case is that the whole water mass is not enough; all water on the planet is contained in the atmosphere because the water mass of the planet is smaller than a certain value determined by the surface temperature. The second case is that liquid water cannot exist thermodynamically on the surface; there is no ocean water by definition when the surface temperature is higher than the critical temperature of water. In these two cases, however, the greenhouse effect of water vapor is not essential; provided that there are enough absorbers (carbon dioxide, for instance), these atmospheric states can emerge even if water vapor is transparent to infrared radiation. These are the cases that are unsuitable for the term "runaway greenhouse."

The third case is the focus of our discussion in this paper. As will be mentioned in the following, it is possible to define an equilibrium state where the oceans cannot exist, not by considering the water mass or the critical point, or both, but by considering the radiation properties of the atmosphere. Infrared absorption of water vapor plays an essential role in evaporating seawater in this case. In the following only this third case, where the ocean cannot exist in an equilibrium state regardless of the water mass or the critical point of water, or both, will be referred to as an atmosphere in a runaway greenhouse state.

The existence of a runaway greenhouse state was demonstrated mathematically by Komabayashi (1967, 1968) and Ingersoll (1969). They found that there is an upper limit of $F^{\uparrow}_{\mathrm{IRtop}}$ to the atmosphere that is in equilibrium with the ocean. This means that when the incident solar flux exceeds the upper limit the atmosphere with the ocean cannot remain in an equilibrium state. The ocean must evaporate regardless of its mass, and the atmosphere will be in a runaway greenhouse state. The model utilized by Ingersoll is quite simple. It consists of only a gray stratosphere in a radiative equilibrium state. The condition of the existence of the ocean is replaced with the assumption that the water vapor at the tropopause is given by saturated water vapor pressure. Komabayashi (1967, 1968) composed a similar simple model but with only one component, assuming a water vapor atmosphere. In what follows, the upper limit of the outgoing infrared radiation obtained by Komabayashi and Ingersoll will be called the Komabayashi–Ingersoll limit.

Further investigations on runaway greenhouse states have recently been carried out using models with more precise radiative and thermodynamic processes and with the area expanded to the troposphere (Kasting 1988; Abe and Matsui 1988). The results of these models indicate that runaway greenhouse states are obtained as a singular behavior of $F^{\uparrow}_{\mathrm{IRtop}}$. The results of Abe and Matsui (1988) showed that when $F^{\uparrow}_{\mathrm{IRtop}}$ reaches around 305 W m$^{-2}$ the atmosphere and ocean cannot coexist in an equilibrium state. The results of Kasting (1988) are similar; in the range of $400 \leqslant T_s \leqslant 1500$ K, $F^{\uparrow}_{\mathrm{IRtop}}$ retains the value of 309 W m$^{-2}$ (Fig. 7, Kasting 1988), which means that $T_s$ will undergo an extreme change at around $F^{\uparrow}_{\mathrm{IRtop}} \sim 300$ W m$^{-2}$ and the ocean will evaporate if the incident solar flux is increased above this value.

By reviewing these studies, it is found that the possibility of the occurrence of a runaway greenhouse state can be investigated by searching for the existence of singularities in the behavior of $F^{\uparrow}_{\mathrm{IRtop}}$, such as an asymptotic value or an upper limit. In the following, we will refer to these singularities as the "radiation limits" of the atmosphere. The atmosphere, which takes in more incoming solar radiation than the radiation limit, can be regarded as in a runaway greenhouse state.

In the following section we will reveal the atmospheric structures by which radiation limits emerge. The existence of an asymptotic value for $F^{\uparrow}_{\mathrm{IRtop}}$, as seen in Abe and Matsui (1988) and Kasting (1988), seems to be what corresponds to the Komabayashi–Ingersoll limit in a more complex model that includes the troposphere. It is unfortunate, however, that the handling of the thermodynamic and radiative processes in those models are all complicated, and it is not easy to follow what is actually happening. In section 2 we will introduce a simple one-dimensional atmospheric model with a stratosphere that is in a radiative equilibrium (as is Ingersoll's) and a troposphere with an appropriate moist adiabatic lapse rate. In section 3 we will try to ascertain what kind of atmospheric structures create a radiation limit. It will be revealed that the origin of the asymptotic limit appearing in Abe and Matsui (1988) and Kasting (1988) is completely different from that of the Komabayashi–Ingersoll limit.

## 2. Model

The model employed here will be described here in detail. It is the so-called one-dimensional radiative–convective equilibrium model. A comparison between the models of Komabayashi (1967, 1968), Ingersoll (1969), Kasting (1988), Abe and Matsui (1988), and our model is summarized in Table 1. The important points are that in our model the stratosphere is in radiative equilibrium similar to Ingersoll (1969) and the radiative and thermodynamic processes of the troposphere are taken into consideration as in Kasting (1988) and Abe and Matsui (1988), though the formulation is extremely simple. The values of parameters used in our calculations are summarized in Table 2.

### *a. Components of the atmosphere*

It is assumed that the atmosphere consists of two components; the noncondensable component and the gas phase of the condensable component. These com-

TABLE 1. A comparison of the models of Komabayashi (1967, 1968), Ingersoll (1969), Kasting (1988), Abe and Matsui (1988), and our model.

| | Komabayahi (1967, 1968) | Ingersoll (1969) | Kasting (1988) | Abe and Matsui (1988) | Our model |
|---|---|---|---|---|---|
| Stratosphere | Radiative equilibrium<br>Water vapor saturated | Radiative equilibrium<br>Constant mole fraction | Isothermal<br>Constant mole fraction | Radiative equilibrium<br>Constant mole fraction* | Radiative equilibrium |
| Tropopause | Not considered | Water vapor saturated | Water vapor saturated | Water vapor saturated* | Water vapor saturated |
| Troposphere | Not considered | Not considered | Saturated<br>Adiabatic lapse rate | Saturated<br>Adiabatic lapse rate | Saturated<br>Adiabatic lapse rate |
| Radiative process | Nonscattering<br>Gray | Nonscattering<br>Gray | Scattering<br>Absorption depends on wavelength | Scattering<br>Absorption depends on wavelength | Nonscattering<br>Gray |
| Components | Ideal gas<br>One component | Ideal gas<br>Two components | Nonideal gas<br>$N_2$, $O_2$, $CO_2$, $H_2O$ | Nonideal gas<br>$CO_2$, $H_2O$ | Ideal gas<br>Two components |
| Critical point | Not treated explicitly | Not treated explicitly | exists (647.1 K) | exists (647.1 K) | None |

* The actual condition was to take the smaller value of either the water vapor mole fraction of the lower layer or the mole fraction of saturated water vapor. The results, however, were shown in the table.

ponents behave as an ideal gas. The condensable component is an imaginary matter whose gas–liquid equilibrium curve will approximate that of actual water. It has liquid and gas phases, but does not have a solid phase. The latent heat per mole, $l$, the mole specific heat of the gas phase of the condensable component, $c_{pv}$, and the mole specific heat of the noncondensable component, $c_{pn}$, are assumed to be constant and independent of temperature. Since $l$ is constant, the specific heat of the liquid phase of the condensable component is equal to $c_{pv}$, and the critical point does not exist.

We further assume that the liquid phase volume is ignored in the Clausius–Clapeyron relationship, which gives the saturation water vapor pressure $p^*$ to be

$$p^*(T) = p_0^* \exp\left(-\frac{l}{RT}\right),$$

where $T$ is temperature, $R$ is the gas constant. The values of $l$ and $p_0^*$ are given here so that $p^*(T)$ will approximate the table and the formula described in Eisenberg and Kauzmann (1961).

We assume that the molecular weight of the noncondensable component $m_n$ is the same as that of the condensable component $m_v$. By this simplification, the average molecular weight $\bar{m}$ becomes independent of the mixing ratio of the noncondensable component, which makes calculations and interpretations easier.

In our model formulation we did not include the existence of the critical point ($T_c$ = 647.1 K) because

TABLE 2. Values of various quantities used in the calculations.

| | |
|---|---|
| **Physical constants** | |
| Gas constants | $R = 8.314$ J mol$^{-1}$ K$^{-1}$ |
| Acceleration of gravity | $g = 9.8$ m s$^{-2}$ |
| The Stefan–Boltzmann constant | $\sigma = 5.67 \times 10^{-8}$ W m$^{-2}$ K$^{-4}$ |
| **Parameters of model** | |
| Molecular weight of noncondensable component | $m_n = 18 \times 10^{-3}$ (kg mol$^{-1}$) |
| Molecular weight of condensable component | $m_v = 18 \times 10^{-3}$ (kg mol$^{-1}$) |
| Mole specific heat at constant pressure of condensable component | $c_{pv} = 4R$ |
| Latent heat of condensable component | $l = 43655$ (J mol$^{-1}$) |
| Constant for the water vapor saturation curve | $p_0^* = 1.4 \times 10^{11}$ (Pa) |
| Mole specific heat at constant pressure of noncondensable component | $c_{pn} = 3.5R$ (sections 3b, 3c, 3e)<br>$c_{pn} = 4.5R$ (section 3d) |
| Amount of noncondensable component at the bottom of atmosphere | $p_{n0} = 10^5$ (Pa) (sections 3b, 3e)<br>$p_{n0} = 10^4 \sim 10^7$ (Pa) (section 3c)<br>$p_{n0} = 10^6 \sim 10^8$ (Pa) (section 3d) |
| Absorption coefficient of condensable component | $\kappa_v = 0.01$ (m$^2$ kg$^{-1}$) (sections 3a–3d)<br>$\kappa_v = 0.01$ or 0 (m$^2$ kg$^{-1}$) (section 3e) |
| Absorption coefficient of noncondensable component | $\kappa_n = 0$ (m$^2$ kg$^{-1}$) (sections 3a–3d)<br>$\kappa_n = 0 \sim 0.01$ (m$^2$ kg$^{-1}$) (section 3e) |

its existence does not seem to affect the asymptotic behavior of $F^{\uparrow}_{\mathrm{IRtop}}$ (Kasting 1988, Fig. 7). In the following, the condensable component will be occasionally called "water," its gas phase "water vapor," and the gas–liquid equilibrium curve will be called the saturated water vapor pressure curve.

*b. Radiative transfer*

The atmosphere is assumed to be transparent to solar radiation. The absorption coefficient of infrared radiation is constant and independent of wavelength (gray). The noncondensable component, however, is transparent except for that in section 3e. The effect of radiation scattering is not considered.

The optical depth $\tau$ is defined by

$$d\tau = (\kappa_v x_v m_v + \kappa_n x_n m_n)\frac{dp}{\bar{m}g}, \tag{1}$$

where $p$ is the pressure, $g$ is the acceleration of gravity, $\kappa_v$ and $\kappa_n$ are the absorption coefficients of the condensable and noncondensable components, respectively, and $x_v^* \equiv p^*(T)/p$ and $x_n$ are the mole fractions of the saturation condensable and the noncondensable components.

The radiation transfer equation is integrated by using the Eddington approximation. The upward and downward radiation flux densities ($F^{\uparrow}_{\mathrm{IR}}$ and $F^{\downarrow}_{\mathrm{IR}}$) can be written as

$$F^{\uparrow}_{\mathrm{IR}}(\tau) = \pi B(\tau) - \int_{\tau_b}^{\tau} \frac{d}{d\tau'}(\pi B(\tau')) \times \exp\left(-\frac{3}{2}(\tau' - \tau)\right)d\tau', \tag{2}$$

$$F^{\downarrow}_{\mathrm{IR}}(\tau) = \pi B(\tau) - \int_{0}^{\tau} \frac{d}{d\tau'}(\pi B(\tau')) \times \exp\left(-\frac{3}{2}(\tau - \tau')\right)d\tau' - \pi B(0)\exp\left(-\frac{3}{2}\tau\right), \tag{3}$$

where $B \equiv \sigma T^4/\pi$ is the blackbody radiation intensity, $\sigma$ is the Stefan–Boltzmann constant, and $\tau_b$ is the optical depth of the entire atmosphere. Note that $F^{\uparrow}_{\mathrm{IRtop}} \equiv F^{\uparrow}_{\mathrm{IR}}(0)$.

*c. Structure of the troposphere*

The troposphere is assumed to be saturated. The temperature lapse rate in the troposphere is assumed to be a moist pseudoadiabatic lapse rate given by

$$\left(\frac{\partial T}{\partial p}\right)_{\substack{\text{moist}\\ \text{pseudoadiabat}}} = \frac{\dfrac{RT}{pc_{pn}} + \dfrac{x_v^*}{x_n}\dfrac{l}{pc_{pn}}}{x_n + x_v^*\dfrac{c_{pv}}{c_{pn}} + \dfrac{x_v^*}{x_n}\dfrac{l^2}{RT^2 c_{pn}}}. \tag{4}$$

The tropopause is determined as follows. Provided that the partial pressure $p_{n0}$ of the noncondensable component at the bottom of the atmosphere and the surface temperature $T_s$ are given, $T(p)$ and $x_v(p)$ are obtained by integrating (4) up to the top of the atmosphere. The net radiation flux convergence can be calculated employing (2) and (3). There appears to be a height where the net convergence becomes positive in the upper levels of the atmosphere, where the temperature is sufficiently low. The position of the tropopause is taken to be this height.

*d. Structure of the stratosphere*

The stratosphere is in a radiative equilibrium. The mole fraction of the condensable component in the stratosphere is constant and is equal to the value at the tropopause. The temperature structure with respect to $\tau$ can be immediately obtained from (2) and (3) with $F^{\uparrow}_{\mathrm{IRtop}}$ as a parameter:

$$\pi B = \frac{1}{2}F^{\uparrow}_{\mathrm{IRtop}}\left(\frac{3}{2}\tau + 1\right). \tag{5}$$

Equation (1) can also be integrated immediately and gives

$$\tau = (\kappa_v x_v m_v + \kappa_n x_n m_n)\frac{p}{\bar{m}g}. \tag{6}$$

$$= [\kappa_v m_v p^*(T_{\mathrm{tp}}) + \kappa_n m_n(p_{\mathrm{tp}} - p^*(T_{\mathrm{tp}}))]\frac{p}{p_{\mathrm{tp}}}\frac{1}{\bar{m}g}, \tag{7}$$

where the subscript "tp" indicates that it is the value at the tropopause. When $\tau$ in (5) is replaced with $p$ by employing (7), the temperature structure of the stratosphere with respect to $p$ is obtained for given $F^{\uparrow}_{\mathrm{IRtop}}$. Here $p_{\mathrm{tp}}$ remains as a parameter: the value of $p_{\mathrm{tp}}$ will be determined when the stratosphere is attached with the troposphere.

Note that if we use $\kappa_n = 0$, then the stratospheric model of Ingersoll is obtained. In the case of $\kappa_n = 0$, (5) and (7) mean that $T$ is a function only of $p/p_{\mathrm{tp}}$, and its functional form is readily determined without any discussion of the tropospheric structure. Furthermore, when $x_n = 0$, the model of Komabayashi is obtained.

## 3. Results and discussions

*a. The Komabayashi–Ingersoll limit*

Let us restrict ourselves to the cases where $\kappa_n = 0$ for the time being. The stratosphere of our model is now exactly the same as that of Ingersoll and, therefore, has the Komabayashi–Ingersoll limit. The derivation of the Komabayashi–Ingersoll limit has been described recently by Goody and Yung (1989). In this section, by reproducing the derivation of the limit, the reason for the existence of the Komabayashi–Ingersoll limit

will be explained in detail, and the value of the Komabayashi–Ingersoll limit of our model will be calculated.

By evaluating (5) and (7) at the tropopause, we have

$$\frac{1}{2} F^{\uparrow}_{\mathrm{IRtop}} \left( \frac{3}{2} \tau_{\mathrm{tp}} + 1 \right) = \sigma T_{\mathrm{tp}}^4, \tag{8}$$

$$\tau_{\mathrm{tp}} = \kappa_v p^*(T_{\mathrm{tp}}) \frac{1}{g} \frac{m_v}{\bar{m}}. \tag{9}$$

In order to eliminate $\tau_{\mathrm{tp}}$ and to obtain $T_{\mathrm{tp}}$, it is convenient to plot (8) and (9) on the $\tau_{\mathrm{tp}}$–$T_{\mathrm{tp}}$ plane. As can be easily seen from Fig. 1, when $F^{\uparrow}_{\mathrm{IRtop}}$ exceeds a certain value, the curves (8) and the curve (9) cannot intersect at all. This value of $F^{\uparrow}_{\mathrm{IRtop}}$ is the Komabayashi–Ingersoll limit. The reason for the appearance of the Komabayashi–Ingersoll limit is now very clear. The amount of absorbent matter (8) required for preserving the radiative equilibrium and the amount of absorbent matter (9) required for preserving the gas–liquid equilibrium cause a contradiction. In order to emit outgoing radiation above the Komabayashi–Ingersoll limit, the atmospheric temperature must be sufficiently high, but the absorbent matter obtained from the gas–liquid equilibrium at that temperature causes the optical thickness to become too thick to allow the required radiation. The cause of this contradiction depends on the shape of the saturated water vapor pressure curve.

The parameters of our model give the value of the Komabayashi–Ingersoll limit to be 385 W m$^{-2}$ and the corresponding tropopause temperature to be 255 K. As clearly seen from (8) and (9), the value of the Komabayashi–Ingersoll limit depends on the choice of parameters. The values obtained by Ingersoll (1969), for instance, range from 321 to 655 W m$^{-2}$.

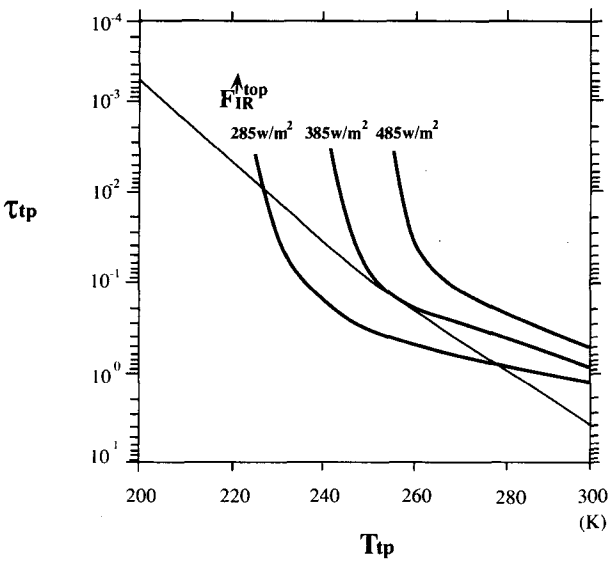


FIG. 1. The relationship between $\tau_{\mathrm{tp}}$ and $T_{\mathrm{tp}}$. The thick lines represent Eq. (8) with $F^{\uparrow}_{\mathrm{IRtop}}$ as a parameter, and the thin line represents Eq. (9).

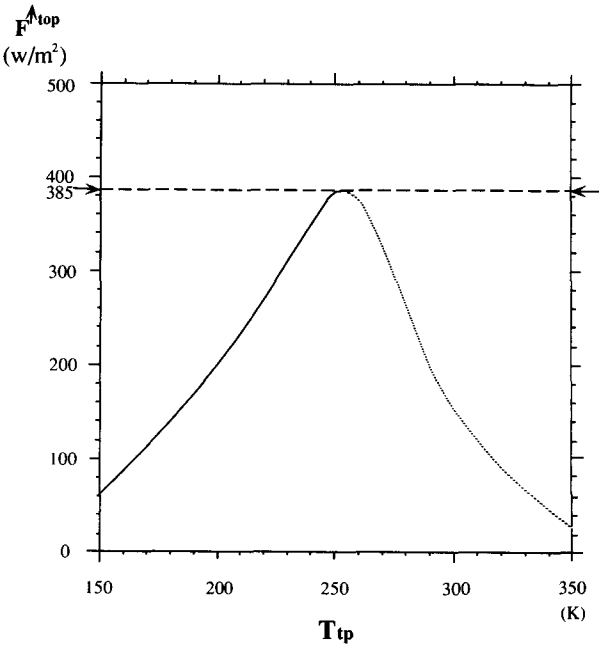


FIG. 2. The relationship between $T_{\mathrm{tp}}$ and $F^{\uparrow}_{\mathrm{IRtop}}$. The Komabayashi–Ingersoll limit of this model is 385 W m$^{-2}$. The branch indicated by the broken line is physically unrealistic.

Figure 2 shows the behavior of $T_{\mathrm{tp}}$ with respect to $F^{\uparrow}_{\mathrm{IRtop}}$. When the value of $F^{\uparrow}_{\mathrm{IRtop}}$ is smaller than the Komabayashi–Ingersoll limit, there are two solutions[1] for $T_{\mathrm{tp}}$. Following Ingersoll's argument, we do not accept the larger $T_{\mathrm{tp}}$ solution, since a supersaturated region exists within the stratosphere. The solution that was not adopted is indicated in Fig. 2 as a dashed line.

The Komabayashi–Ingersoll limit is an extremely strong limit in the sense that its existence does not depend on the tropospheric structure. If only the stratosphere is in a radiative equilibrium and its bottom is saturated, this limit will appear. The only condition that hints at the tropospheric structure is that the tropopause is saturated. The saturation condition can be weakened to the condition that the relative humidity is given at the tropopause. Let $h$ be the relative humidity. The equation (9) has only to be rewritten as

$$\tau_{\mathrm{tp}} = \kappa_v h p^*(T_{\mathrm{tp}}) \frac{1}{g} \frac{m_v}{\bar{m}}, \tag{10}$$

by which the same argument holds. For a fixed $h < 1$, there is a limit value of $F^{\uparrow}_{\mathrm{IRtop}}$. In order to eliminate the Komabayashi–Ingersoll limit by adjusting the absorbent matter, it is required that the tropopause condition is slackened to (10), and moreover, the tem-

[1] More precisely, there are three solutions; the remaining one is located at extremely large $T_{\mathrm{tp}}$.

perature dependency of $h$ counteracts the temperature dependency of $p^* \sim \exp(-l/RT)$. In other words, a dynamic process that will cause an extremely dry stratosphere must exist.

Finally, we have to note here that the derivation of the Komabayashi–Ingersoll limit depends on the fact that the relationships between the absorbent matter and temperature are represented extremely simply. In case the infrared absorption coefficient depends on the wave length, that is, the atmosphere is not gray, the amount of absorbent matter cannot be determined by such a simple method as indicated in Fig. 1.

### b. *The relationship between $F^{\uparrow}_{IRtop}$ and $T_s$ when $p_{n0} = 10^5$ Pa*

Now let us determine the equilibrium structure that includes the troposphere. In this section the partial pressure $p_{n0}$ of the noncondensable component at the bottom of the atmosphere is fixed to be $10^5$ Pa, which is the same value as Kasting's (1988). This value is roughly equal to the current earth's surface pressure. We still keep $\kappa_n = 0$ in this section.

The calculated relationship between $T_s$ and $F^{\uparrow}_{IRtop}$ is shown in Fig. 3. The vertical structures of the mole fraction and the temperature are shown in Fig. 4 and Fig. 5. In Fig. 4 the vertical coordinate is taken as pressure $p$, while in Fig. 5 it is the optical depth $\tau$.

The important points in Fig. 3 are the following two items. The first is that the maximum of $F^{\uparrow}_{IRtop}$ does not reach the Komabayashi–Ingersoll limit. The second is that the value of $F^{\uparrow}_{IRtop}$ tends to be constant (about 293 W m$^{-2}$) when the surface temperature is above 400 K. In our model $F^{\uparrow}_{IRtop}$ has an asymptotic value

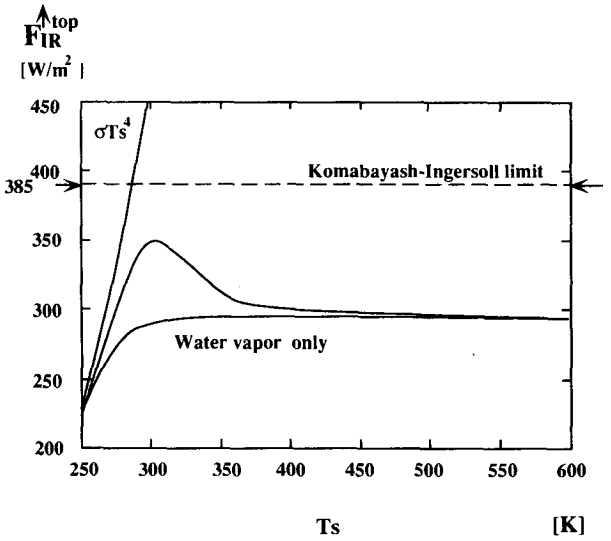


FIG. 3. The relationship between $T_s$ and $F^{\uparrow}_{IRtop}$ for the case when $P_{n0} = 10^5$ Pa. $F^{\uparrow}_{IRtop}$ for the case of the saturation water vapor atmosphere, the blackbody radiation $\sigma T_s^4$, and the Komabayashi–Ingersoll limit are also indicated.

in the same manner as those of Abe and Matsui (1988) and Kasting (1988).

Let us observe the characteristics of Fig. 3 in detail. Figure 5 shows that the optical depth of the entire atmosphere goes above unity as $T_s$ exceeds 300 K. Hence, when $T_s$ is sufficiently above 300 K, $F^{\uparrow}_{IRtop}$ is not directly related to $T_s$ but to the temperature structure around $\tau = 1$. Therefore, to understand the relationship between $T_s$ and $F^{\uparrow}_{IRtop}$, it is necessary to study the changes in the temperature structure near $\tau = 1$ with the changes of $T_s$. From Fig. 4a it is seen that as $T_s$ becomes high, the temperature structure $T = T(p)$ approaches the saturated water vapor pressure curve $T = T^*(p)$. Correspondingly, the mole fraction of the water vapor approaches unity (Fig. 4b). In order to see the role of this temperature structure to $F^{\uparrow}_{IRtop}$ it is necessary to translate this into the structure seen from the optical depth $T = T(\tau)$. Equation (1), however, indicates that $\tau = \kappa_v p/g$ at the limit $x_v \to 1$. Therefore, even when the temperature structure is seen from the $\tau$ coordinate, the tendency of temperature structure to approach a certain curve is unchanged. Actually, in Fig. 5a it is depicted that the temperature distribution with regard to $\tau$ approaches a limiting curve as $T_s$ increases. As a result, the temperature structure in the vicinity of $\tau = 1$, which determines the value of $F^{\uparrow}_{IRtop}$, does not depend on $T_s$.

In order to ascertain the foregoing discussion, the relationship between $T_s$ and $F^{\uparrow}_{IRtop}$, of which the atmosphere consists only of the water vapor, is indicated in Fig. 3. This is the case when the temperature and the water vapor distribution are given exactly by the saturated water vapor pressure curve. It is clearly seen that the asymptotic value of $F^{\uparrow}_{IRtop}$ is reproduced by this water vapor atmosphere.

From Fig. 3, it is possible to determine the reason that causes the upper and the lower limits of $F^{\uparrow}_{IRtop}$. It is the magnitude of the tropospheric lapse rate around $\tau \sim 1$. First of all, for a fixed $T_s$, the value of $F^{\uparrow}_{IRtop}$ determined from the water vapor atmosphere is the lower limit of $F^{\uparrow}_{IRtop}$. Secondly, $F^{\uparrow}_{IRtop}$ decrease as $T_s$ increases for $T_s > 300$ K, where $\tau_s > 1$. It should be noted that in both cases $F^{\uparrow}_{IRtop}$ decreases as the water vapor content increases. According to (2), $F^{\uparrow}_{IRtop}$ is represented as the integrated value of the gradient of the thermal radiation $B$ with respect to $\tau$, and hence, $F^{\uparrow}_{IRtop}$ becomes smaller as $dT/d\tau$ is decreased. Let us ignore the contribution of the stratosphere. The average value of the moist adiabatic lapse rate $dT/dp$ becomes smaller as the mole fraction of the water vapor becomes larger. This trend becomes even stronger for the lapse rate with respect to the optical depth, $dT/d\tau$, since the optical depth per mass $d\tau/dp$ becomes large as the mole fraction of the water vapor increases. Thus, the increase of water vapor causes smaller $dT/d\tau$, which results in smaller $F^{\uparrow}_{IRtop}$.

Regarding the asymptotic behavior of $F^{\uparrow}_{IRtop}$, Kasting (1988) explains that in such a temperature range

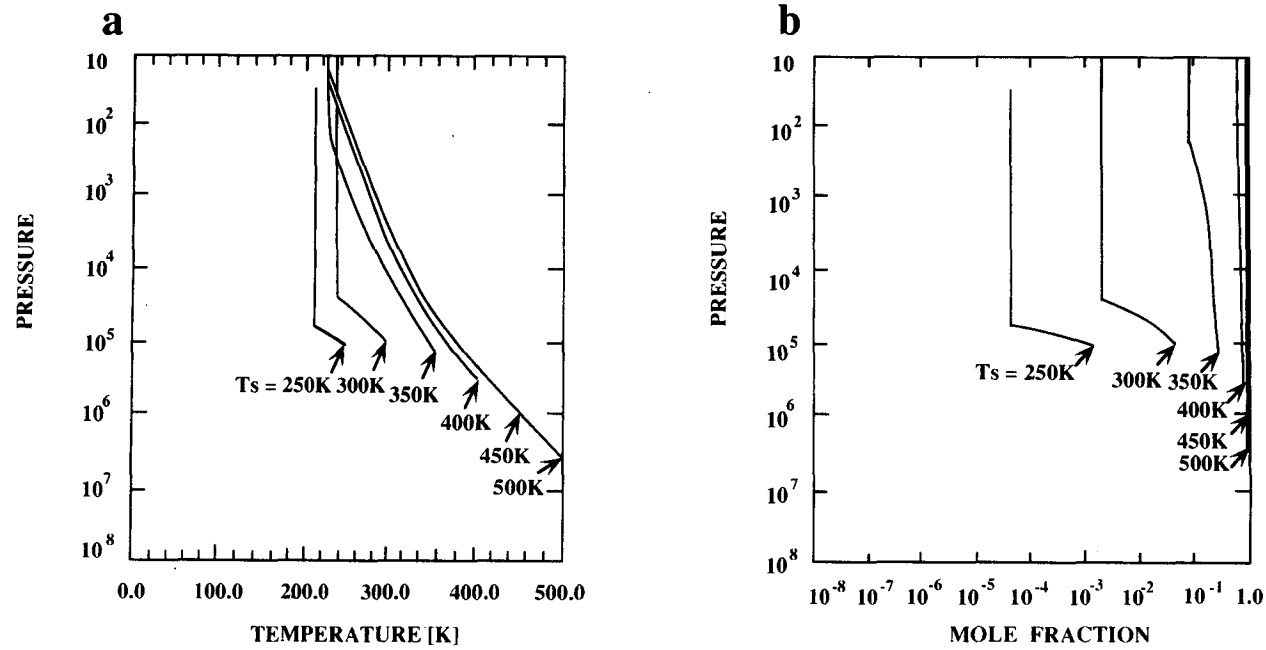


FIG. 4. The relationships between $p$ and (a) $T$ and (b) $x_v$.

the moist convective layer becomes thicker and the atmosphere becomes opaque for the whole infrared spectrum. Only the atmospheric region whose pressure is below 0.2 ~ 0.3 bar will permit the emission into outer space. Therefore, even when the convective layer becomes thicker as $T_s$ increases, it has no influence on the outgoing infrared radiation. Kasting has also pointed out that the temperature structure approaches the saturated water vapor pressure curve. This tendency is also pointed out by Abe and Matsui (1988). These

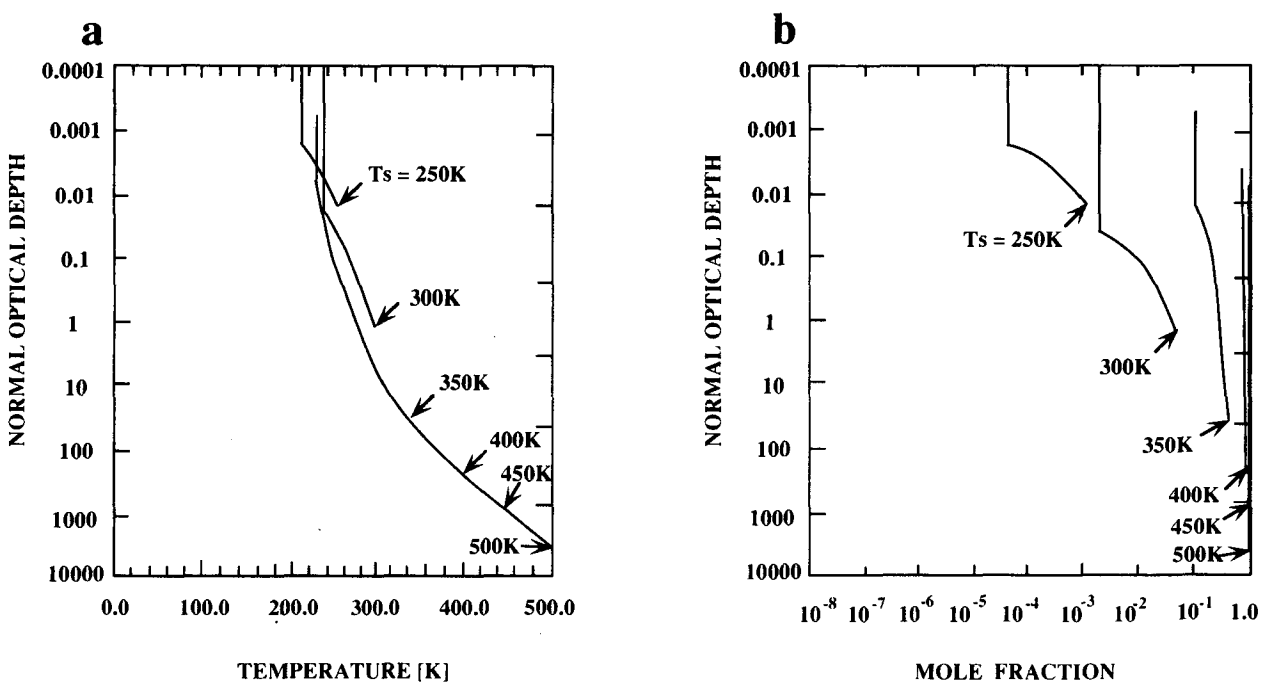


FIG. 5. The relationships between $\tau$ and (a) $T$ and (b) $x_v$.

explanations, however, describe only half of the mechanism. What is really important is that the temperature structure of the region is fixed with respect to $\tau$. Regarding the radiative process, they do not attribute any meaning to the asymptotic temperature structure.

When $F_0$ is between 353 and 293 W m$^{-2}$, there are two solutions of the radiative equilibrium. One is a solution in which the tropopause pressure is high, $T_s$ is low, and $x_v$ is small; the other is a solution in which the tropopause pressure is low, $T_s$ is high, and $x_v$ is large. In these two solutions both temperature $T_{tp}$ and optical depth $\tau_{tp}$ at the tropopause are equal. Note that these two solutions correspond to the same point in Fig. 2. It should be also noted that discussion of the stability of these two solutions is beyond the scope of the present model. One might be tempted to imagine that equilibrium solutions on the branch where $F^{\uparrow}_{IRtop}$ decreases against the increase of $T_s$ are unstable (for example, Komabayashi 1967). The argument often runs like this: provided that the incoming solar flux is fixed, a slight increase in $T_s$ would lead to a decrease in outgoing IR and, hence, to a further increase in surface temperature. Such arguments, however, contain two implicit assumptions. First is that we have specified the equations that govern the dynamic behavior of the system around the steady states; that is, the atmosphere–ocean system is in an "equilibrium state" even when it does not balance with the incoming heat flux. This assumption is accepted only after consideration of time constants of the related physical processes. It is quite possible that a slight increase in $T_s$ leads to an increase of $F^{\uparrow}_{IRtop}$, since *it takes a little bit of time* to establish the temperature and moisture structure that would be in balance with the new $T_s$, and hence, the stratosphere is warmed and the tropospheric height is decreased. The second assumption is that the initial perturbation of $T_s$ can build up without any difficulty. This is not obvious because the perturbation is not a zero-energy disturbance; that is, we need extra energy to build it up.

### c. *The relationship between $F^{\uparrow}_{IRtop}$ and $T_s$ when $p_{n0}$ is changed: The Komabayashi–Ingersoll limit with the troposphere*

It is suggested in the previous section that the value of $F^{\uparrow}_{IRtop}$ increases as the water vapor amount decreases. In the following, we will change the partial pressure $p_{n0}$ of the noncondensable component at the bottom of the atmosphere and realize the situations where the mole fraction of water vapor is changed. The other conditions are the same as in section 3b.

Figure 6 indicates the relationship between $T_s$ and $F^{\uparrow}_{IRtop}$ for various $p_{n0}$. It can be perceived that, at the same value of $T_s$, $F^{\uparrow}_{IRtop}$ actually increases as $p_{n0}$. For a fixed $T_s$, the larger $p_{n0}$ means the smaller mole fraction of the water vapor at each height, and therefore, the lapse rate $dT/dp$ and also $dT/d\tau$ are larger. In Fig. 6, at $p_{n0} = 10^7$ Pa the maximum value of $F^{\uparrow}_{IRtop}$ reaches the Komabayashi–Ingersoll limit. Conversely, when $p_{n0}$ is small, the saturated water vapor curve controls $F^{\uparrow}_{IRtop}$ at lower temperature, and $F^{\uparrow}_{IRtop}$ approaches the asymptotic value of the water vapor atmosphere more easily.

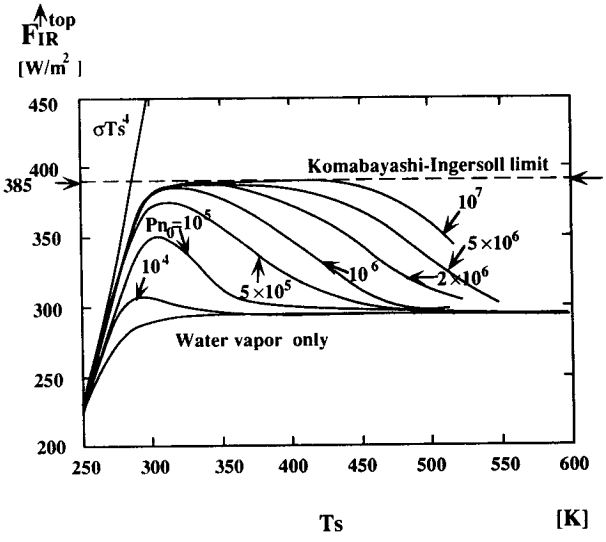


FIG. 6. The relationships between $T_s$ and $F^{\uparrow}_{IRtop}$ when $p_{n0}$ is changed. $F^{\uparrow}_{IRtop}$ for the case of the saturation water vapor atmosphere, the blackbody radiation $\sigma T_s^4$, and the Komabayashi–Ingersoll limit are also indicated.

Calculations show that, for a fixed $T_s$, the optical depth of the entire atmosphere decreases as $p_{n0}$ increases (not shown). The entire optical depth for $p_{n0} = 10^8$ Pa is about one-half of that for $p_{n0} = 10^4$ Pa. This is because the smaller water vapor mole fraction caused by the large $p_{n0}$ gives the larger lapse rate. Consequently, the vertically averaged atmospheric temperature is lowered, and the amount of the water vapor is decreased.

### d. *The relationship between $F^{\uparrow}_{IRtop}$ and $T_s$ when $c_{pn}$ is made large: Another radiation limit*

As seen in the previous sections, $F^{\uparrow}_{IRtop}$ increases as the lapse rate of the troposphere increases. As the mole fraction of the water vapor decreases, the moist adiabatic lapse rate approaches the dry adiabatic lapse rate, but it cannot exceed this value. Therefore, there should be an upper limit of $F^{\uparrow}_{IRtop}$ determined by the dry adiabatic lapse rate. The reason why the Komabayashi–Ingersoll limit is observed in Fig. 6 should be that the Komabayashi–Ingersoll limit is smaller than the possible upper limit determined by the dry adiabatic lapse rate. In order to have a larger value of the dry adiabatic lapse rate and hence a smaller value of the possible upper limit, the calculations in this section were made with $c_{pn} = 4.5\ R$.

Figure 7 shows the relationship between $T_s$ and $F^{\uparrow}_{IRtop}$. All the values of $F^{\uparrow}_{IRtop}$ in Fig. 7 are lower than the Komabayashi–Ingersoll limit. The behavior of $F^{\uparrow}_{IRtop}$ clearly suggests that there exists an upper limit other than the Komabayashi–Ingersoll limit. An investigation of the solutions shows that the mole fraction of water vapor is extremely low (under $10^{-3}$) in the neighborhood of $\tau = 1$ and that the lapse rate can be regarded as dry adiabatic.

The reason why $F^{\uparrow}_{IRtop}$ is almost constant over a certain range of $T_s$ when $p_{n0}$ is increased is basically the same as the reason for the asymptotic value mentioned earlier. The temperature structure with respect to $\tau$ around $\tau \sim 1$ becomes independent of $T_s$. Substituting $x_v = p^*/p$ into (1) and ignoring the effect of stratosphere, the optical depth is given by

$$\tau(p) = -\int_p^0 \kappa_v \frac{p^*}{p'} \frac{m_v}{\bar{m}g}\, dp'. \qquad (11)$$

The independent variable can be replaced from $p$ to $T$ by regarding the tropospheric temperature as the dry adiabatic lapse rate:

$$\tau(T) = -\int_T^0 \kappa_v \frac{p^*}{RT'} c_{pn} \frac{m_v}{\bar{m}g}\, dT'. \qquad (12)$$

It can be seen from (12) that the temperature structure is written in the form of $T = T(\tau)$, and consequently, the temperature determined exclusively if only the optical depth is given. Hence, when the atmosphere is sufficiently thick and there is no surface contribution to $F^{\uparrow}_{IRtop}$, then $F^{\uparrow}_{IRtop}$ does not depend on $T_s$ but becomes constant.

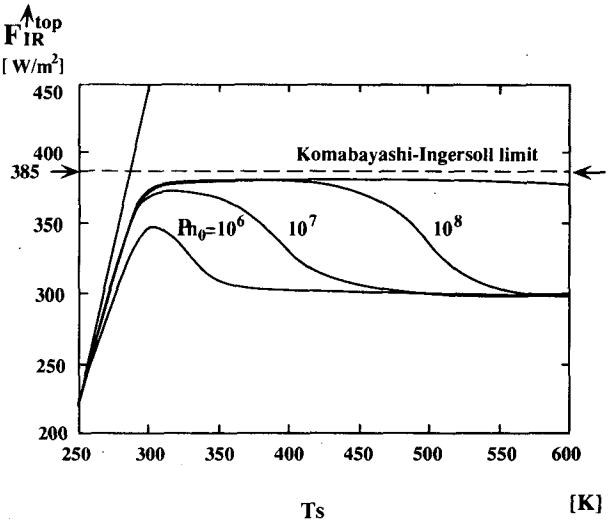


FIG. 7. The relationships between $T_s$ and $F^{\uparrow}_{IRtop}$ when $c_{pn}$ is increased to be $4.5R$. The values of $p_{n0}$ are $10^6$ Pa, $10^7$ Pa, and $10^8$ Pa. The blackbody radiation $\sigma T_s^4$ and the Komabayashi–Ingersoll limit are also indicated.

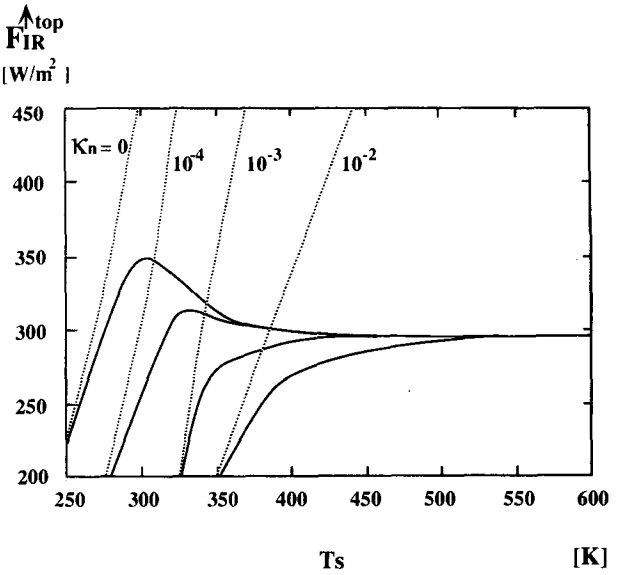


FIG. 8. The relationships between $T_s$ and $F^{\uparrow}_{IRtop}$ when the noncondensable component absorbs infrared radiation. The solid lines indicate the cases when the absorption coefficient of the noncondensable component $\kappa_n$ is 0.0, 0.0001, 0.001, and 0.01 $m^2\ kg^{-1}$, respectively. The dashed lines indicate the cases where the condensable component is transparent ($\kappa_v = 0\ m^2\ kg^{-1}$).

### e. *The relationship between $F^{\uparrow}_{IRtop}$ and $T_s$ when the noncondensable component absorbs infrared radiation*

It was assumed up to the previous section that the noncondensable component was transparent to infrared radiation. In this section the effects of the noncondensable component on infrared absorption will be considered.

Figure 8 shows the results of calculations with $p_{n0} = 10^5$ Pa when $\kappa_n$ is increased from 0 to 0.01 $m^2\ kg^{-1}$. The case of $\kappa_n = 0\ m^2\ kg^{-1}$ is the same as that described in section 3b. The interesting point of Fig. 8 is that the maximum value of $F^{\uparrow}_{IRtop}$, which appears around $T_s = 300 \sim 350$ K, becomes smaller and eventually disappears as the absorption due to the noncondensable component becomes stronger. This is simply because when $T_s$ is fixed the increase of absorption reduces $F^{\uparrow}_{IRtop}$. At high values of $T_s$, however, the asymptotic value of $F^{\uparrow}_{IRtop}$ remains, as in the cases where the noncondensable component is transparent, since the asymptotic value appears as the atmosphere approaches the structure composed only of the condensable component.

The behavior of $F^{\uparrow}_{IRtop}$ shown in Fig. 8 is informative in understanding the results of the previous studies. Both Abe and Matsui (1988) and Kasting (1988) give asymptotic values of $F^{\uparrow}_{IRtop}$ similar to that of our model. In their models, however, a maximum of $F^{\uparrow}_{IRtop}$, like that indicated in our earlier figures, does not exist, or if it does, the value is extremely small. From the results

shown here it is considered that the reason why the maximum values are small is because they include the absorption due to carbon dioxide. The fact that a small maximum appears in Kasting (1988) while no maximum is found in Abe and Matsui (1988) is explained by the difference of the noncondensable component. As the noncondensable component, Kasting (1988) considered the actual air, while Abe and Matsui (1988) considered pure carbon dioxide. The noncondensable component composed of pure carbon dioxide has a larger absorption coefficient than that of the actual air.

Finally, let us consider a complete reversal situation to what we have assumed up to the present section. Let us assume that the condensable component (water vapor) is transparent ($\kappa_v = 0$ m$^2$ kg$^{-1}$). The broken line in Fig. 8 describes the relationship between $F^{\uparrow}_{\mathrm{IRtop}}$ and $T_s$ in such a case. Even when the surface temperature becomes high, $F^{\uparrow}_{\mathrm{IRtop}}$ does not approach any constant values. We have to note that even in this case the temperature structure with respect to $p$ approaches the saturation vapor curve as $T_s$ increases (not shown). For the same value of $\kappa_n$, there are hardly any differences of the atmospheric structure between the solid-line ($\kappa_v \neq 0$) and the broken-line ($\kappa_v = 0$) cases of Fig. 8. As discussed in section 3b, in order to have an asymptotic value of $F^{\uparrow}_{\mathrm{IRtop}}$, the atmospheric structure with regard to $\tau$ should become fixed. Only that the temperature structure approaches the saturation vapor curve is insufficient.

## 4. Concluding remarks

There are restrictions on the infrared radiation $F^{\uparrow}_{\mathrm{IRtop}}$ that can be emitted from the top of a gray atmosphere, that has a saturated troposphere and a radiative equilibrium stratosphere:

1) $F^{\uparrow}_{\mathrm{IRtop}}$ cannot exceed the blackbody radiation $\sigma T_s^4$ that corresponds to the surface temperature $T_s$. This is the thin limit of the optical thickness of the atmosphere.

2) $F^{\uparrow}_{\mathrm{IRtop}}$ cannot exceed the Komabayashi–Ingersoll limit. The Komabayashi–Ingersoll limit is the upper limit of $F^{\uparrow}_{\mathrm{IRtop}}$ emitted from a radiative equilibrium stratosphere that has a constant mole fraction of water vapor and a saturated tropopause.

3) When the optical thickness of the entire atmosphere is sufficiently larger than unity,

(i) $F^{\uparrow}_{\mathrm{IRtop}}$ is larger than the value obtained for the saturation water vapor atmosphere where the atmosphere is composed only of the saturated water vapor,

(ii) $F^{\uparrow}_{\mathrm{IRtop}}$ is smaller than the value obtained for the atmosphere whose lapse rate is almost equal to the dry adiabat. This is the case when the mole fraction of water vapor in the atmosphere is extremely small.

The existence of an upper limit and a lower limit of $F^{\uparrow}_{\mathrm{IRtop}}$ is caused by the fact that the moist adiabatic lapse rate is larger than the lapse rate determined by the saturation water vapor pressure curve and smaller than the dry adiabatic lapse rate. These limiting values do not depend on $p_{n0}$ or $T_s$. This is because the temperature structure can be written only in terms of the optical thickness; that is, $T = T(\tau)$. Such a functional relationship between $T$ and $\tau$ is obtained when the temperature structure approaches a gas–liquid equilibrium curve that is represented only as a function of pressure, $T = T(p)$, and, moreover, when the amount of the condensable component (that is, the absorption matter) is determined only by pressure and the optical depth can be represented only as a function of pressure, $\tau = \tau(p)$.

According to these restrictions for $F^{\uparrow}_{\mathrm{IRtop}}$, the radiation limit of the atmosphere is determined in the following way. At the extreme low limit of $T_s$, $F^{\uparrow}_{\mathrm{IRtop}}$ is almost equal to the upper limit of item 1. When the surface temperature is at its high limit, the mole fraction of water vapor becomes unity, so $F^{\uparrow}_{\mathrm{IRtop}}$ approaches the lower limit defined in item 3a. When the optical thickness of the entire atmosphere becomes sufficiently larger than unity, but the mole fraction of water vapor is sufficiently smaller than 1, the smaller of either the Komabayashi–Ingersoll limit (item 2) or the dry adiabatic limit (item 3b) appears. The region where $F^{\uparrow}_{\mathrm{IRtop}}$ does not depend on $T_s$, which appears in the results of Abe and Matsui (1988) and Kasting (1988), corresponds to that indicated in item 3a and is different from the Komabayashi–Ingersoll limit. The runaway greenhouse state appears when the radiation limit of $F^{\uparrow}_{\mathrm{IRtop}}$ exists and the incident solar flux is larger than this limit.

There is a possibility that the foregoing conclusion greatly depends on the fact that the radiation model is gray. For the existence of an asymptotic value of $F^{\uparrow}_{\mathrm{IRtop}}$, it is important that the temperature structure can be written in the form of $T = T(\tau)$ for large $\tau$. Even if the radiation is not gray, there is a good evidence that such an equation may be obtained, since, despite the fact that the radiation processes of Abe and Matsui (1988) and Kasting (1988) are not gray, their models exhibit a region where $F^{\uparrow}_{\mathrm{IRtop}}$ does not depend on $T_s$. The reason for the correspondence of their results and those presented here is that in such high temperature and high pressure the continuous absorption band of water vapor comes to predominate and its absorption characteristic becomes close to that of the gray absorber.

*Acknowledgments.* The authors wish to express their thanks to all participants in the *Seminar on the Structures of the Planetary Atmospheres* held at the Geophysical Institute of the University of Tokyo. The thoughtful comments by the anonymous reviewers are

greatly appreciated. The authors also wish to thank Ms. Tabata for preparing the figures. Calculations were performed at the Computer Centre of the University of Tokyo and Computer Center of Nagoya University. The terminal program ETERM, developed by Drs. Kohketsu and Takano of the Earthquake Research Institute, University of Tokyo, was employed.

## REFERENCES

Abe, Y., 1988: Conditions required for water-ocean formation on an earth-sized planet. *Lunar Planet Science XIX,* Lunar Planet Institute, 1–2.

——, and T. Matsui, 1988: Evolution of an impact-generated $H_2O$–$CO_2$ atmosphere and formation of a hot proto-ocean on earth. *J. Atmos. Sci.,* **45,** 3081–3101.

Eisenberg, D., and W. Kauzmann, 1969: *The Structure and Properties of Water.* Oxford University Press, 302 pp.

Gold, T., 1964: Outgassing process on the Moon and Venus. *The Origin and Evolution of Atmospheres and Oceans.* P. J. Brancazio and A. G. W. Cameron, Eds., Wiley and Sons, 249–256.

Goody, R. M., and Y. L. Yung, 1989: *Atmospheric Radiation. Theoretical Basis,* 2nd ed. Oxford University Press, 519 pp.

Ingersoll, A. P., 1969: The runaway greenhouse: A history of water on Venus. *J. Atmos. Sci.,* **26,** 1191–1198.

Kasting, J. F., 1988: Runaway and moist greenhouse atmospheres and the evolution of Earth and Venus. *Icarus,* **74,** 472–494.

Komabayashi, M., 1967: Discrete equilibrium temperatures of a hypothetical planet with the atmosphere and the hydrosphere of one component-two phase system under constant solar radiation. *J. Meteor. Soc. Japan,* **45,** 137–139.

——, 1968: Conditions for the coexistence of the atmosphere and the oceans. *Shizen,* **23,** No. 2, 24–31 (in Japanese).

Plass, G. N., 1961: The influence of infrared absorptive molecules on the climate. *Ann. New York Acad. Sci.,* **25,** 61–71.